J. Fluid Mech. (1991), *vol.* 228, *pp.* 1–24
Printed in Great Britain

Frontogenesis driven by horizontally quadratic distributions of density

By DAVID JACQMIN
NASA Lewis Research Center, Cleveland, OH 44135, USA

(Received 22 November 1989 and in revised form 3 October 1990)

Experiments by Simpson & Linden (1989) have shown that a horizontally nonlinear distribution of fluid density is necessary in order to produce frontogenesis. This paper considers the simplest case of such a nonlinear distribution, a quadratic density distribution in a channel. Two flow models are examined, porous media and Boussinesq. The evolution equations for both these flows can be reduced to one-dimensional systems. An exact solution is derived for porous-media flow with no molecular diffusion. Numerical solutions are shown for the other cases. The porous-media and inviscid/non-diffusive Boussinesq systems exhibit 'classic' frontogenesis behaviour: a rapid and intense steepening of the density gradient near the lower boundary while horizontal divergence reduces the upper-boundary density gradient to nearly zero. The viscous Boussinesq system exhibits a more complicated behaviour. In this system, boundary-layer effects force frontogenesis away from the lower boundary and at late times the steepest density gradients are close to mid-channel. One feature of these model systems is that they can exhibit blow-up in finite time. Proof of blow-up is given for the non-diffusive porous media and inviscid/nondiffusive Boussinesq cases. Numerical results indicate that blow-up also occurs for the diffusive porous-media case and that it may occur for the diffusive Boussinesq case. Despite the blow-up we believe that the model solutions can be applied to real situations. To support this a two-dimensional calculation has been made of Boussinesq frontogenesis in a long box. This calculation shows close agreement with the corresponding one-dimensional calculation up to times close to blow-up.

1. Introduction

Simpson & Linden (1989) have recently conducted experiments to examine the onset and causes of frontogenesis. Their experimental set-up was a long rectangular box filled with fluid with a controlled initial horizontal density distribution. The fluid, initially motionless, was set into motion by gravity. They found both analytically and experimentally that fronts fail to form when the initial gradient of density is uniform. The introduction of step discontinuities in the initial density gradient (making the density distribution piecewise linear instead of linear), however, did lead to frontal formation. These results led Simpson & Linden to conclude that curvature must be present in their experiment's initial density field in order for a front to form. They further hypothesized that the timescale of frontogenesis is on the order of $((g/\bar{\rho})L\rho_{xx})^{-\frac{1}{2}}$. Here, ρ_{xx} and $\bar{\rho}$ are the characteristic density 'curvature' and the mean density over a region of size L.

This paper discusses some flow models that are applicable to Simpson & Linden's experiment and that can be used to examine the onset and timescales of frontogenesis.

We consider a fluid with an initially horizontally constant $\rho_{xx}(z)$ in a channel or semi-infinite enclosure. The exact form of the initial density distribution is $\rho = \rho_0 + \frac{1}{2}\rho_{xx}x^2$. This density distribution results in a comparatively simple mathematical problem for two commonly used flow models: flow in porous media and Boussinesq flow. In both cases the initially quadratic distribution of density remains quadratic. The corresponding horizontal velocity is linear in x and the vertical velocity is x-independent. The originally two-dimensional system can thus be reduced to a one-dimensional set of evolution equations for quantities dependent on t and z.

There is also a secondary application of our results. Flows that will be considered here can exhibit blow-up in finite time. As it happens, blow-up of solutions of the Euler and Navier–Stokes equations has recently been a topic of interest. Stuart (1987) has considered the blow-up of three-dimensional stagnation flows and Childress *et al.* (1989) have shown that blow-up can occur in two dimensions. Both Stuart and Childress *et al.*, as in this paper, considered unbounded domains with velocity fields that change linearly in certain directions. Childress *et al.* concluded that these blow-ups are due primarily to the unboundedness of the model flows' initial vorticity. The results herein, in showing that even the porous-media model allows blow-up, seem to support this. We also believe, however, that our Boussinesq model is usefully applicable to the Simpson & Linden experiment for times short of blow-up. Two-dimensional calculations will be presented to try to show this.

This paper considers porous-media flow and Boussinesq flow separately. We first consider the simpler case of porous-media flow. Though frontogenesis in porous media is not itself of direct concern, the wealth of results that can be derived for it (many analytic results are possible) make this is a useful model problem. In the section on Boussinesq flow we consider both inviscid/non-diffusive and viscous/diffusive cases. As mentioned, we also test the usefulness of the one-dimensional Boussinesq results by making a comparison to a full two-dimensional simulation of flow in a long box.

2. The porous-media case

In this section we consider porous-media flow in a semi-infinite enclosure of height $2H$. The equations of flow are

$$\frac{\partial u}{\partial x} + \frac{\partial w}{\partial z} = 0, \tag{2.1a}$$

$$u = -k\frac{\partial p}{\partial x}, \tag{2.1b}$$

$$w = -k\left(\frac{\partial p}{\partial z} + g\rho\right), \tag{2.1c}$$

$$\frac{\partial \rho}{\partial t} + u\frac{\partial \rho}{\partial x} + w\frac{\partial \rho}{\partial z} = D\left(\frac{\partial^2 \rho}{\partial x^2} + \frac{\partial^2 \rho}{\partial z^2}\right), \tag{2.1d}$$

with boundary conditions

$$w(z = \pm H) = \left.\frac{\partial \rho}{\partial z}\right|_{z=\pm H} = 0, \quad u(x = 0) = \left.\frac{\partial \rho}{\partial x}\right|_{x=0} = 0. \tag{2.1e}$$

In the above, x and z are the horizontal and vertical coordinates, u and w the corresponding velocities, and ρ the density. k is the 'resistance' (permeability divided by the product of porosity and absolute viscosity) to flow and D is the diffusivity of ρ.

The equations can be non-dimensionalized by scaling density by A_ρ (to be defined later), lengths by H, velocities by $A_\rho kg$, pressure by $A_\rho Hg$, and time by $H/A_\rho kg$. The rescaled equations are

$$\frac{\partial u}{\partial x}+\frac{\partial w}{\partial z}=0, \tag{2.2a}$$

$$u=-\frac{\partial p}{\partial x}, \tag{2.2b}$$

$$w=-\left(\frac{\partial p}{\partial z}+\rho\right), \tag{2.2c}$$

$$\frac{\partial \rho}{\partial t}+u\frac{\partial \rho}{\partial x}+w\frac{\partial \rho}{\partial z}=R_D\left(\frac{\partial^2 \rho}{\partial x^2}+\frac{\partial^2 \rho}{\partial z^2}\right), \tag{2.2d}$$

where $R_D = D/A_\rho Hkg$. The boundary conditions (2.1e) are now applied at $z=\pm 1$.

We now set $\rho=\rho_0+\rho_2 x^2$, $p=p_0+p_2 x^2$, $u=u_1 x$, and $w=w_0$, where $\rho_0, \rho_2, p_0, p_2, u_1$, and w_0 are functions of z and t. This leads to two sets of one-dimensional equations. The main set, for ρ_2, p_2, u_1, and w_0, is

$$u_1+\frac{\partial w_0}{\partial z}=0, \tag{2.3a}$$

$$u_1=-2p_2, \tag{2.3b}$$

$$\frac{\partial p_2}{\partial z}=-\rho_2, \tag{2.3c}$$

$$\frac{\partial \rho_2}{\partial t}+2u_1\rho_2+w_0\frac{\partial \rho_2}{\partial z}=R\frac{\partial^2 \rho_2}{\partial z^2}. \tag{2.3d}$$

A subsidiary set, for ρ_0 and p_0, is forced by w_0 and ρ_2.

Equations (2.3) can be reduced to a single evolution equation for w_0. ρ_2 can be expressed in terms of w_0 as $\rho_2=-\frac{1}{2}\partial^2 w_0/\partial z^2$. Equation (2.3$d$) becomes

$$\frac{\partial}{\partial t}\frac{\partial^2 w_0}{\partial z^2}+w_0\frac{\partial^3 w_0}{\partial z^3}-2\frac{\partial w_0}{\partial z}\frac{\partial^2 w_0}{\partial z^2}=R_D\frac{\partial^4 w_0}{\partial z^4}. \tag{2.4}$$

Boundary conditions for w_0 are that $w_0=\partial^3 w_0/\partial z^3=0$ at $z=\pm 1$.

At this point we can define the density scale A_ρ. We impose

$$\int_{-1}^{+1}\rho_{2,\mathrm{nondim}}(z,t=0)\,\mathrm{d}z=1.$$

Thus A_ρ is defined from the magnitude of the initial distribution of dimensional ρ_2:

$$A_\rho=H\int_{-H}^{+H}\rho_2^*(z^*,t^*=0)\,\mathrm{d}z^*,$$

where * indicates dimensional quantities. This scaling will also be used for the Boussinesq case. The porous-media timescaling, in terms of $\rho^*_{x^*x^*}$, becomes

$$\left(\tfrac{1}{2}kg\int_{-H}^{+H}\rho^*_{x^*x^*}(z^*, t^*=0)\,\mathrm{d}z^*\right)^{-1}.$$

In terms of $\overline{\rho^*_{x^*x^*}}$, the average of $\rho^*_{x^*x^*}$, this is $(kgH\overline{\rho^*_{x^*x^*}}(t^*=0))^{-1}$.

2.1. *Blow-up in finite time*

When $R_D = 0$, it can be proved that an interesting 'flaw' exists in this model system's behaviour – it blows up in finite time. The proof requires that initially $\rho \geqslant 0$ and stably distributed ($\mathrm{d}\rho/\mathrm{d}z \leqslant 0$) and depends on the fact that $\partial w_0/\partial z$ is then limited to being both convex and monotonically decreasing in z for all t. The proof is detailed in Appendix A and will just be outlined here.

The proof is based on the evolution equation for $\partial w_0/\partial z$ at the lower boundary. Because of its convexity and monotonicity $\partial w_0/\partial z$ is always greatest there. From integration of (2.4) the evolution equation for $\partial w_0/\partial z$ is

$$\frac{\partial}{\partial t}\frac{\partial w_0}{\partial z} + w_0\frac{\partial^2 w_0}{\partial z^2} - \frac{3}{2}\left(\frac{\partial w_0}{\partial z}\right)^2 = h(t), \tag{2.5}$$

where $h(t)$ is the constant of integration. $h(t)$ adjusts with time to ensure that the boundary conditions on w_0 are met. It can be found in terms of $\partial w_0/\partial z$ by integrating (2.5). This yields

$$h(t) = -\frac{5}{4}\int_{-1}^{+1}\left(\frac{\partial w_0}{\partial z}\right)^2 \mathrm{d}z. \tag{2.6}$$

The evolution equation for $\partial w_0/\partial z$ at the lower boundary is

$$\frac{\partial}{\partial t}\frac{\partial w_0}{\partial z}\bigg|_{-1} = \frac{3}{2}\left(\frac{\partial w_0}{\partial z}\bigg|_{-1}\right)^2 + h(t). \tag{2.7}$$

Appendix A proves blow-up by bounding $h(t)$ above $-\alpha(\partial w_0/\partial z|_{-1})^2$, where α is less than $\frac{3}{2}$. Somewhat lengthy arguments based on the convexity and monotonicity of $\partial w_0/\partial z$ result in

$$\int_{-1}^{+1}\left(\frac{\partial w_0}{\partial z}\right)^2 \mathrm{d}z < 0.7114\left(\frac{\partial w_0}{\partial z}\bigg|_{-1}\right)^2. \tag{2.8}$$

Applying (2.8) to (2.7) and solving the resulting ordinary differential inequality then gives

$$t_\mathrm{b} < \left(0.6107\,\frac{\partial w_0}{\partial z}\bigg|_{-1,\,t=0}\right)^{-1}, \tag{2.9}$$

where t_b is the time to blow-up. It can also be shown, again from the convexity of $\partial w_0/\partial z$ and from the definition of A_ρ, that $\partial w_0/\partial z|_{-1,\,t=0} \geqslant 1$. Thus t_b is bounded globally below 1.6375.

Blow-up will be shown to occur also for the inviscid/non-diffusive Boussinesq case and it appears to occur for both the porous media and Boussinesq diffusive cases. Questions that arise are: Does this behaviour indicate our approach is invalid? Are any of these solutions actually applicable to real situations? We will later attempt to allay such concerns by making a comparison to a 'realistic' two-dimensional calculation. Also, some related fluid-flow models have exhibited singularities but have nonetheless been found useful. In particular, Hoskins & Bretherton's (1972)

model of frontogenesis in a rotating quasi-geostrophic fluid also has quadratic distributions of density (this time in the y-direction, the direction parallel to the front) and, by their description, their solutions 'collapse' at finite time on the lower boundary. Nevertheless, they feel that their solutions are realistic and that their model's more important limitation is its inability to account for turbulent transport. This becomes of significant importance for front development well before their model's blow-up.

Another related model problem is that of Childress *et al.* (1989). They have recently considered the blow-up of incompressible stagnation-point flows which have linear distributions of vorticity. The geometry they assumed was, as here, the infinite channel. The problems they considered actually make up a subset of the Boussinesq case that we will consider in §3. They found many examples of blow-up and concluded that singularities form 'as a result of the unboundedness of initial vorticity' (p. 5). What happens in the systems considered herein is that quadratic distributions of density act as a source for linear distributions of vorticity that then lead to blow-up.

2.2. R_D *zero: analytic solutions*

Childress *et al.* discuss a solution technique for their inviscid model problem which we now apply to (2.5). Their inviscid model equation differs from (2.5) only in having a coefficient of 1 multiplying $(\partial w_0/\partial z)^2$ instead of $\frac{3}{2}$.

Following Childress *et al.*, we work with Lagrangian coordinates $\tau = t$ and ζ. The evolution equation for $\partial w_0/\partial z$ becomes

$$\frac{\partial}{\partial \tau}\left(\frac{\partial w_0}{\partial z}\right) - \frac{3}{2}\left(\frac{\partial w_0}{\partial z}\right)^2 = h(\tau). \tag{2.10}$$

The equation for ρ_2 is

$$\frac{\partial \rho_2}{\partial \tau} - 2\frac{\partial w_0}{\partial z}\rho_2 = 0. \tag{2.11}$$

The transformation from ζ to z is given by

$$z(\zeta) = -1 + \int_{-1}^{\zeta} J(\eta, \tau)\, \mathrm{d}\eta, \tag{2.12}$$

where $J = \partial z/\partial \zeta$ is the Jacobian. The evolution equation for J, obtained from $\mathrm{D}\zeta/\mathrm{D}t = 0$, is

$$\frac{\partial J}{\partial \tau} - \frac{\partial w_0}{\partial z} J = 0. \tag{2.13}$$

The initial condition on $J(\zeta)$ is that it is equal to one. From (2.12), J is subject to the constraint

$$\int_{-1}^{+1} J\, \mathrm{d}\zeta = 2. \tag{2.14}$$

Equation (2.10) is of Ricatti type. The substitution $\partial w_0/\partial z = -\frac{2}{3}(\partial \phi/\partial \tau)/\phi$ yields the linear equation

$$\frac{\partial^2 \phi}{\partial \tau^2} + \tfrac{3}{2} h(\tau)\, \phi = 0. \tag{2.15}$$

The initial conditions on ϕ can be set to

$$\phi(\zeta, \tau = 0) = 1, \quad \left.\frac{\partial \phi}{\partial \tau}\right|_{\zeta, \tau = 0} = -\frac{3}{2}\left.\frac{\partial w_0}{\partial z}\right|_{\zeta, \tau = 0}. \tag{2.16}$$

From (2.11) and (2.13) and the various initial conditions, $\rho_2 = \rho_2(\zeta, \tau = 0)\phi^{-\frac{4}{3}}$ and $J = \phi^{-\frac{2}{3}}$.

The advantage of the linear equation (2.15) is that it is separable. The solution for ϕ can be expressed in terms of any of its two linearly independent solutions. For example, setting

$$\phi_1(0) = 1, \quad \left.\frac{\mathrm{d}\phi_1}{\mathrm{d}\tau}\right|_0 = 0, \quad \phi_2(0) = 0, \quad \left.\frac{\mathrm{d}\phi_2}{\mathrm{d}\tau}\right|_0 = 1 \tag{2.17}$$

then

$$\phi(\zeta, \tau) = \phi_1(\tau) - \frac{3}{2}\left.\frac{\partial w_0}{\partial z}\right|_{\zeta, \tau=0} \phi_2(\tau). \tag{2.18}$$

A self-contained system of equations for determining ϕ_1 and ϕ_2 is given by the Wronskian equation

$$\phi_1 \frac{\mathrm{d}\phi_2}{\mathrm{d}\tau} - \frac{\mathrm{d}\phi_1}{\mathrm{d}\tau}\phi_2 = 1 \tag{2.19}$$

coupled with the integral constraint equation (2.14):

$$\int_{-1}^{+1} \left(\phi_1(\tau) - \frac{3}{2}\left.\frac{\partial w_0}{\partial z}\right|_{\zeta, \tau=0} \phi_2(\tau)\right)^{-\frac{2}{3}} \mathrm{d}\zeta = 2. \tag{2.20}$$

This approach avoids having to find $h(\tau)$.

We now discuss the particular case of ρ_2 initially independent of z. This is the simplest case and it is also the case most relevant to the experiments of Simpson & Linden. (The flow evolution for this initial condition will be discussed for the Boussinesq model as well.) From the definition of A_ρ, the initial value of ρ_2 is constrained to be $\frac{1}{2}$. Thus

$$\left.\frac{\partial w_0}{\partial z}\right|_{\zeta, \tau=0} = -\zeta, \phi = \phi_1 + \tfrac{3}{2}\phi_2\zeta, \quad \rho_2 = \tfrac{1}{2}(\phi_1 + \tfrac{3}{2}\phi_2\zeta)^{-\frac{4}{3}}.$$

Integrations of ρ_2 then yield

$$w_0 = -\frac{4}{3\phi_2^2}[(\phi_1 + \tfrac{3}{2}\phi_2\zeta)^{-\frac{2}{3}} - \phi_{\mathrm{B}}^{-\frac{2}{3}}] + \frac{2}{3\phi_2^2}(\phi_{\mathrm{T}}^{-\frac{2}{3}} - \phi_{\mathrm{B}}^{-\frac{2}{3}})(z+1), \tag{2.21a}$$

$$\frac{\partial w_0}{\partial z} = \frac{4}{3\phi_2}(\phi_1 + \tfrac{3}{2}\phi_2\zeta)^{-1} + \frac{2}{3\phi_2^2}(\phi_{\mathrm{T}}^{-\frac{2}{3}} - \phi_{\mathrm{B}}^{-\frac{2}{3}}). \tag{2.21b}$$

In the above

$$\phi_{\mathrm{B}} = \phi_1 - \tfrac{3}{2}\phi_2, \quad \phi_{\mathrm{T}} = \phi_1 + \tfrac{3}{2}\phi_2; \tag{2.22}$$

ϕ_{B} and ϕ_{T} are the values of ϕ at the bottom and top boundaries. From $J = \phi^{-\frac{2}{3}}$ and equation (2.12)

$$z = -1 + \frac{2}{\phi_2}[(\phi_1 + \tfrac{3}{2}\phi_2\zeta)^{\frac{1}{3}} - \phi_{\mathrm{B}}^{\frac{1}{3}}]. \tag{2.23}$$

$z(\zeta)$ can be easily inverted to find $\zeta(z)$:

$$\zeta = \frac{2}{3\phi_2}\left[\left(\phi_{\mathrm{B}}^{\frac{1}{3}} + \frac{\phi_2}{2}(z+1)\right)^3 - \phi_1\right]. \tag{2.24}$$

What remains is to find ϕ_1, ϕ_2, ϕ_{B}, and ϕ_{T} in terms of $\tau = t$.

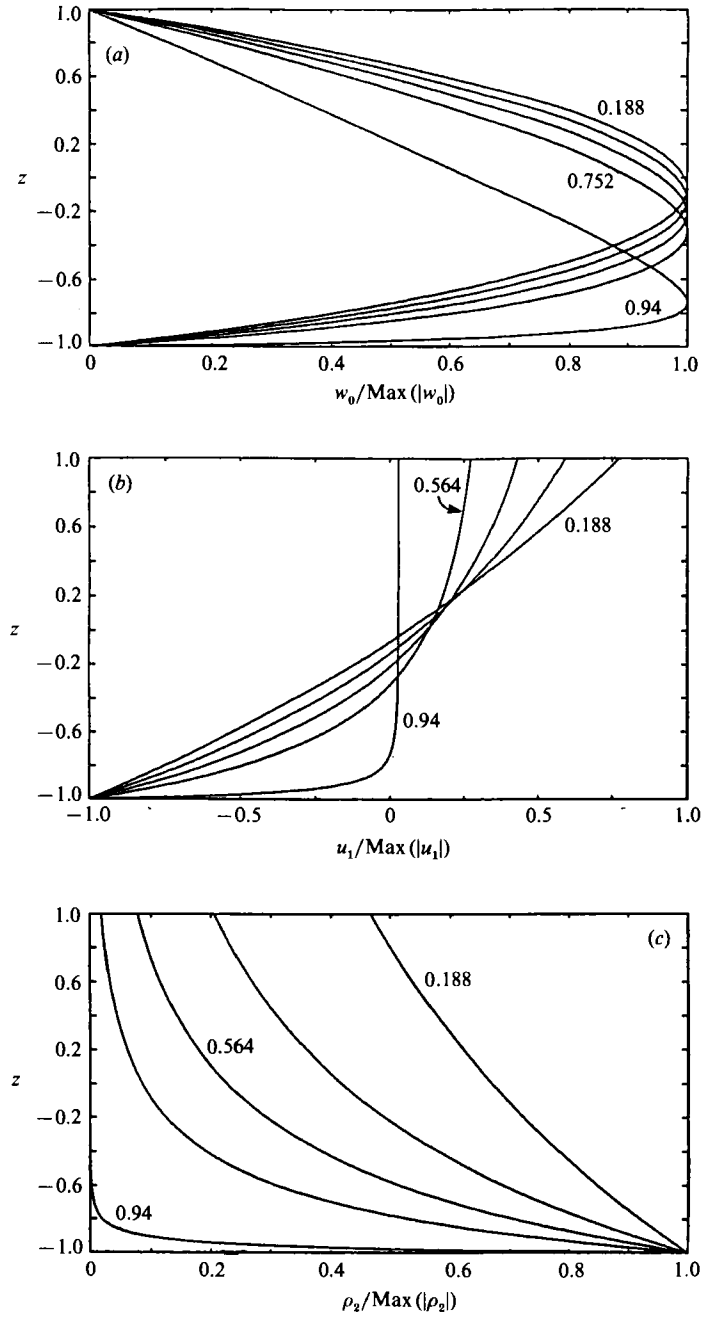

FIGURE 1. The non-diffusive porous-media case with ρ_2 initially uniform. Scaled (*a*) w_0, (*b*) u_1, and (*c*) ρ_2 are shown at time intervals of 0.188, from $t = 0.188$ to 0.94.

To do that, (2.20) is first evaluated to find the relationship between ϕ_1 and ϕ_2. This yields

$$\phi_2 = (\phi_1 + \tfrac{3}{2}\phi_2)^{\frac{1}{3}} - (\phi_1 - \tfrac{3}{2}\phi_2)^{\frac{1}{3}}. \tag{2.25}$$

This can be easily manipulated to find ϕ_T in terms of ϕ_B:

$$\phi_T = [(3 - \tfrac{3}{4}\phi_B^{\frac{2}{3}})^{\frac{1}{2}} - \tfrac{1}{2}\phi_B^{\frac{1}{3}}]^3. \tag{2.26}$$

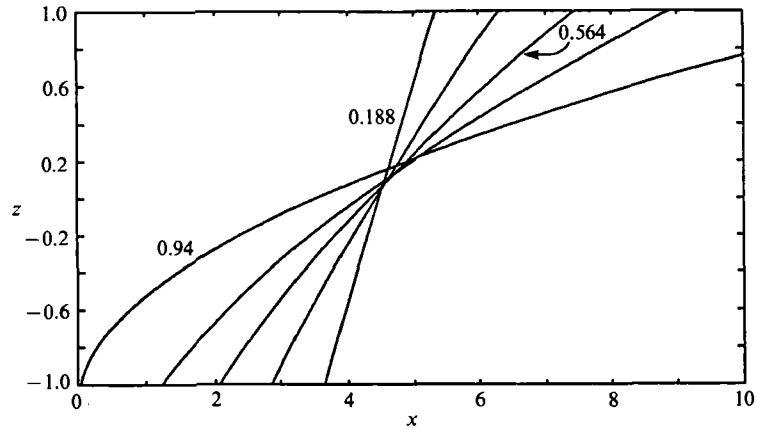

FIGURE 2. The non-diffusive porous-media case with ρ_2 initially uniform. The contour $\rho-\rho_0 = \rho_2 x^2 = 10$ is shown in the $\{x, z\}$ coordinates of the channel. Times shown are at intervals of 0.188 from $t = 0.188$ *to* 0.94.

Then, from the Wronskian equation for ϕ_T and ϕ_B,

$$\frac{d\phi_B}{d\tau} = -\frac{(3-\frac{3}{4}\phi_B^{\frac{2}{3}})^{\frac{1}{2}}}{((3-\frac{3}{4}\phi_B^{\frac{2}{3}})^{\frac{1}{2}}-\frac{1}{2}\phi_B^{\frac{1}{3}})^2}. \tag{2.27}$$

Finally, (2.27) can be integrated to yield

$$\tau = \sqrt{3}\pi-\tfrac{9}{2}-6\sqrt{3}\sin^{-1}(\tfrac{1}{2}\phi_B^{\frac{1}{3}})+(3-\tfrac{3}{4}\phi_B^{\frac{2}{3}})^{\frac{1}{2}}(3\phi_B^{\frac{1}{3}}-\tfrac{1}{2}\phi_B)+\tfrac{3}{4}\phi_B^{\frac{4}{3}}. \tag{2.28}$$

Thus, ϕ_B is expressed implicitly in terms of τ and, from (2.22) and (2.26), ϕ_1, ϕ_2 and ϕ_T are expressible in terms of ϕ_B.

We first consider the time at which the flow blows up. From the transformation between $\partial w_0/\partial z$ and ϕ, blow-up will occur when either $\partial\phi/\partial\tau \to \infty$ or $\phi \to 0$. The integral constraint on J, equation (2.14), and its $\phi^{-\frac{2}{3}}$ form together act, however, to limit the approach to blow-up to the latter. From (2.10) blow-up occurs first at the lower boundary and from (2.15)–(2.16) ϕ has its minimum there. Either leads to the conclusion that the time of blow-up, t_b can be found from just the evolution of ϕ_B. From (2.27), ϕ_B is monotonically decreasing in τ. Thus, from $t = 0$ to t_b ϕ_b varies from one to zero. From (2.28),

$$t_b = \sqrt{3}\pi-\tfrac{9}{2} \approx 0.9414. \tag{2.29}$$

At t_b itself the blow-up is confined to the lower boundary. At the upper boundary, for example, ϕ is $3^{\frac{3}{2}}$ and thus ρ_2 there is only $\frac{1}{18}$. However, $h(t)$ also blows up at t_b and so the blow-up propagates instantly. The transformation between $\partial w_0/\partial z$ and ϕ is invalid past t_b.

Figure 1 shows the evolution of w_0, u_1, and ρ_2. The fields are shown at time intervals of 0.188 up to $t = 0.94$. At each time shown, the fields are normalized to have a maximum value of one. Thus, only their form is shown. The figure shows that evolution of the flow is at first gradual. One of the characteristics of frontogenesis is the formation of an intense lower-boundary current. This becomes noticeable for this flow starting at about $t = 0.6$. Before that, u_1 in the lower half of the channel exhibits approximately uniform shear. In late times, the boundary current becomes extremely narrow and, concomitantly, the position of the maximum of w_0 drops rapidly. Figure 2 tracks the evolution of the contour $\rho-\rho_0 = \rho_2 x^2 = 10$. This, unlike figure 1(*c*), can be directly compared to experiments. The density profile is approximately linear

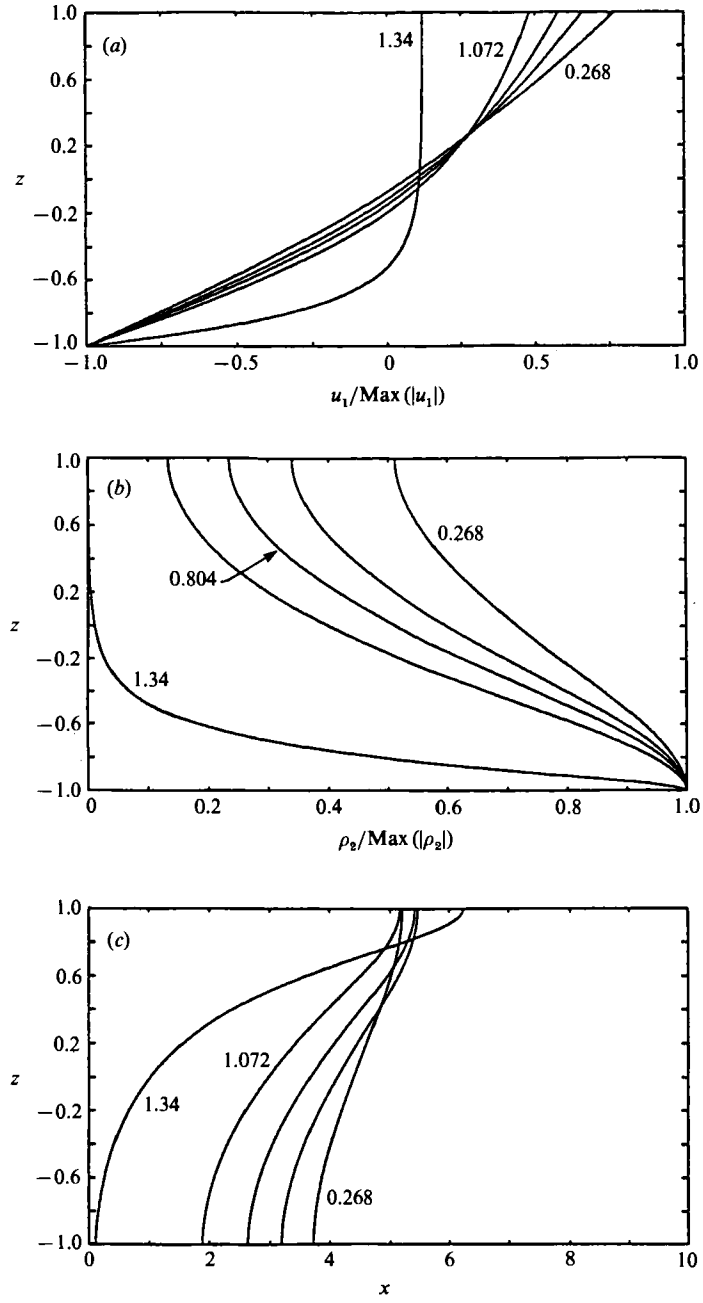

FIGURE 3. The diffusive porous-media case with ρ_2 initially uniform. Scaled (*a*) u_1 and (*b*) ρ_2 and the contour (*c*) $\rho - \rho_0 = \rho_2 x^2 = 10$ are shown at time intervals of 0.268, from $t = 0.268$ to 1.34.

until about $t = 0.7$. The parabolic profile of density shown in Simpson & Linden's experiments is achieved only very near to blow-up.

2.3. R_D *non-zero*

We briefly consider the case $R_D \neq 0$. For the most part, this case must be attacked numerically. Calculations have been made for a wide range of R_D. A fine grid

(500–1000 points) was used with second-order spatial discretizations. Temporal discretization was also second order. The Crank–Nicholson method was used for diffusive terms while convective terms were treated explicitly. Time-step sizes were adaptively selected during the course of calculations so as to always satisfy numerical convective stability criteria.

Most calculations have been made for the case of ρ_2 initially uniform. A particular result, for $R_D = 1$, is shown in figure 3. The figure shows u_1, ρ_2 and the contour $\rho_2 x^2 = 10$ at equal time intervals up to $t = 1.34$, which is just before the flow blows up. The large diffusivity of this flow results in a much thicker lower-boundary current than for the non-diffusive case. The density boundary condition is important on the upper boundary but seems to be ovewhelmed by the frontogenesis process on the lower.

Numerical results for initially uniform ρ_2 have so far yielded blow-up for all R_D. The numerical t_B have been tested by varying both grid sizes and time-step size selection criteria. Convergence to a definite t_B was found as grid spacing and time-step size were reduced. The boundary-layer singularity associated with $R_D \to 0$ seems to be very weak. Calculations for a sequence of small R_D showed a smooth progression of t_B and of the interior flow to the non-diffusive case. The weak effect of the no-flux boundary condition ($\partial^3 w_0/\partial z^3 = 0$) is in great contrast to the effects of the no-slip condition ($\partial w_0/\partial z = 0$) in Childress *et al.*'s stagnation-point flow model. As will be seen in the section on the Boussinesq model, the no-slip condition can completely change the late-time behaviour of a flow.

Efforts to prove blow-up have been unsuccessful. It is easy, however, to prove a much weaker but still significant result; that $\bar{\rho}_2$, the z-averaged value of ρ_2, increases in time monotonically for any stably stratified initial condition. Integrating (2.4) in z yields

$$\frac{\partial}{\partial t}\bar{\rho}_2 = \frac{3}{8}\left(\frac{\partial w_0}{\partial z}\right)^2\Bigg|_{\mathrm{T}}^{\mathrm{B}}. \tag{2.30}$$

The monotonic decrease and convexity of $\partial w_0/\partial z$ in z can be shown to extend to the diffusive case. From that, and from the fact that the z-integral of $\partial w_0/\partial z$ is zero, the right-hand side of (2.30) must be $\geqslant 0$. The right-hand side is zero only when ρ_2 is uniform. Then it can be shown that $\partial^2\bar{\rho}_2/\partial t^2$ is positive.

3. The Boussinesq case

We now consider Boussinesq flow. The domain of flow is a channel of height $2H$. The flow equations are

$$\frac{\partial u}{\partial x} + \frac{\partial w}{\partial z} = 0, \tag{3.1a}$$

$$\frac{\partial u}{\partial t} + u\frac{\partial u}{\partial x} + w\frac{\partial u}{\partial z} = -\frac{\partial p}{\partial x} + \nu\left(\frac{\partial^2 u}{\partial x^2} + \frac{\partial^2 u}{\partial z^2}\right), \tag{3.1b}$$

$$\frac{\partial w}{\partial t} + u\frac{\partial w}{\partial x} + w\frac{\partial w}{\partial z} = -\frac{\partial p}{\partial z} + \nu\left(\frac{\partial^2 w}{\partial x^2} + \frac{\partial^2 w}{\partial z^2}\right) - g\rho, \tag{3.1c}$$

$$\frac{\partial \rho}{\partial t} + u\frac{\partial \rho}{\partial x} + w\frac{\partial \rho}{\partial z} = D\left(\frac{\partial^2 \rho}{\partial x^2} + \frac{\partial^2 \rho}{\partial z^2}\right), \tag{3.1d}$$

with boundary conditions

$$w(z=\pm H)=u(z=\pm H)=\left.\frac{\partial\rho}{\partial z}\right|_{z=\pm H}=0. \tag{3.2}$$

Because of symmetries in the model flow, solutions are also applicable to a semi-infinite enclosure with no-stress sidewall conditions:

$$u(x=0)=\left.\frac{\partial w}{\partial x}\right|_{x=0}=\left.\frac{\partial\rho}{\partial x}\right|_{x=0}=0. \tag{3.3}$$

Equation (3.1) is non-dimensionalized by scaling density by A_ρ, lengths by H, pressure by $A_\rho gH$, velocities by $(A_\rho gH)^{\frac{1}{2}}$, and time by $(H/A_\rho g)^{\frac{1}{2}}$. As with the porous-media case, we set $\rho=\rho_0+\rho_2 x^2$, $p=p_0+p_2 x^2$, $u=u_1 x$ and $w=w_0$. The evolution equations for ρ_2, p_2, u_1, and w_0 are

$$u_1+\frac{\partial w_0}{\partial z}=0, \tag{3.4a}$$

$$\frac{\partial u_1}{\partial t}+u_1^2+w_0\frac{\partial u_1}{\partial z}=-2p_2+R_\nu\frac{\partial^2 u_1}{\partial z^2}, \tag{3.4b}$$

$$\frac{\partial p_2}{\partial z}=-\rho_2, \tag{3.4c}$$

$$\frac{\partial\rho_2}{\partial t}+2u_1\rho_2+w_0\frac{\partial\rho_2}{\partial z}=R_D\frac{\partial^2\rho_2}{\partial z^2}, \tag{3.4d}$$

where $R_\nu=\nu/(A_\rho gH^3)^{\frac{1}{2}}$ and $R_D=D/(A_\rho gH^3)^{\frac{1}{2}}$. The equations for ρ_0 and p_0 form a subsidiary set that is forced by w_0 and ρ_2. Equations (3.4) can be reduced to

$$\frac{\partial}{\partial t}\frac{\partial w_0}{\partial z}+w_0\frac{\partial^2 w_0}{\partial z^2}-\left(\frac{\partial w_0}{\partial z}\right)^2=R_\nu\frac{\partial^3 w_0}{\partial z^3}+2p_2, \tag{3.5a}$$

$$\frac{\partial}{\partial t}\frac{\partial p_2}{\partial z}+w_0\frac{\partial^2 p_2}{\partial z^2}-2\frac{\partial w_0}{\partial z}\frac{\partial p_2}{\partial z}=R_D\frac{\partial^3 p_2}{\partial z^3}. \tag{3.5b}$$

As with the porous-media case, A_ρ is defined by setting

$$\int_{-1}^{+1}\rho_2(z,t=0)\,\mathrm{d}z=1.$$

In terms of $\overline{\rho^*_{x^*x^*}}$, the dimensional z-averaged second horizontal derivative of ρ, the timescaling becomes $(gH\overline{\rho^*_{x^*x^*}})^{-\frac{1}{2}}$. This is essentially the same as the scaling proposed by Simpson & Linden. R_ν and R_D become, respectively, $\nu/[gH^5\overline{\rho^*_{x^*x^*}}(t=0)]^{\frac{1}{2}}$ and $D/[gH^5\overline{\rho^*_{x^*x^*}}(t=0)]^{\frac{1}{2}}$.

3.1. *Inviscid non-diffusive flow*

This section considers both theory and numerical results. Discussion is limited to flows that are initially motionless and that are initially stably stratified.

Appendix B discusses some of the general characteristics of the flow behaviour and presents a proof of blow-up. The result is

$$\left.\frac{\partial}{\partial t}\frac{\partial w_0}{\partial z}\right|_{-1}>0.2886\left(\left.\frac{\partial w_0}{\partial z}\right|_{-1}\right)^2+1. \tag{3.6}$$

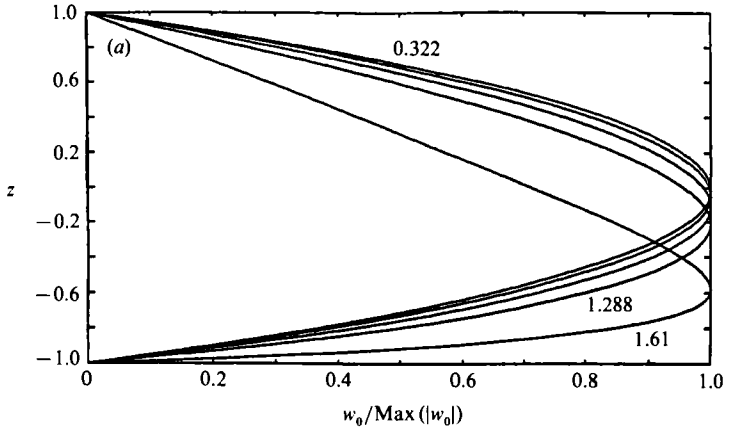

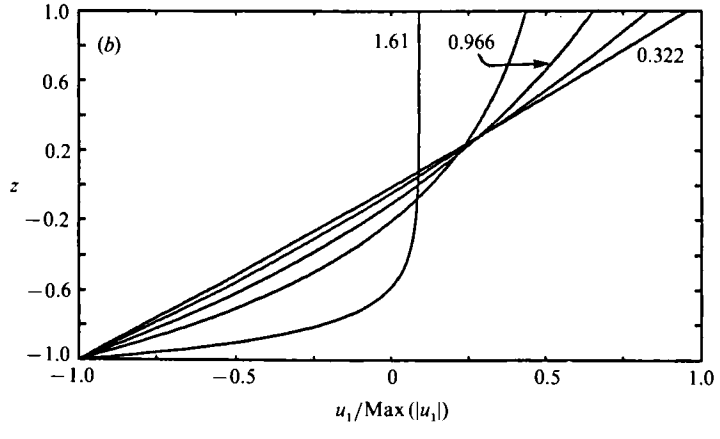

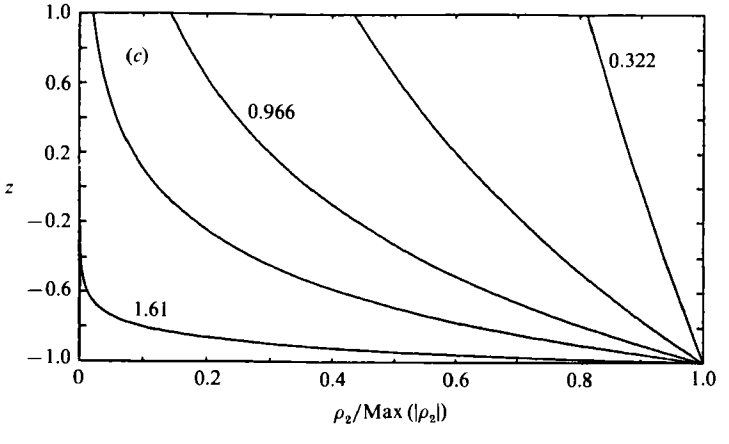

FIGURE 4 (*a–c*). For caption see facing page.

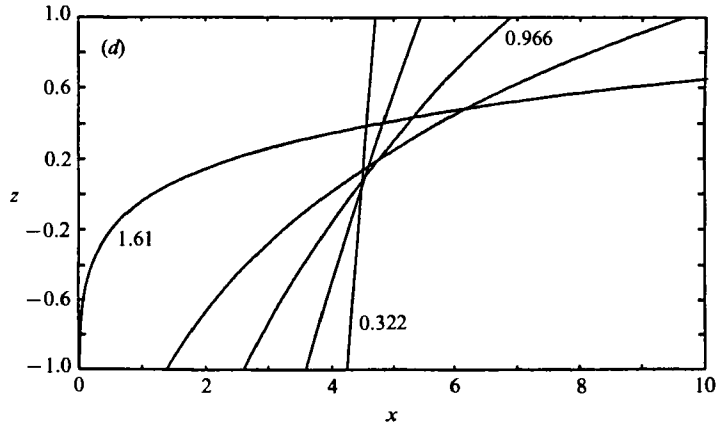

FIGURE 4. The inviscid–non-diffusive Boussinesq case with ρ_2 initially uniform. Scaled (*a*) w_0, (*b*) u_1, and (*c*) ρ_2 and (*d*) the contour $\rho - \rho_0 = \rho_2 x^2 = 10$ are shown at time intervals of 0.322, from $t = 0.322$ to 1.61.

For the initially motionless case this yields

$$t_b < \frac{1}{(0.2886)^{\frac{1}{2}}} \frac{\pi}{2} \approx 2.924. \tag{3.7}$$

The result is a bit weaker than for the porous-media case because the proof does not take much advantage of either the growth or distribution of ρ_2. The proof can be changed in minor ways so that it can be applied to some cases of stagnation-point flow considered by Childress *et al.* Blow-up can be proved for their model when $\partial w_0/\partial z$ is initially convex and initially $\partial^2 w_0/\partial z^2 \leqslant 0$.

We briefly consider the particular case of flow starting from initially uniform ρ_2. Results of numerical calculations are given in figure 4, which shows w_0, u_1, ρ_2 and the contour $\rho_2 x^2 = 10$ at time intervals of 0.322: t_b for this flow is about 1.613. The overall flow behaviour is similar to the porous-media case. As with that case, u_1 at first exhibits approximately uniform shear. A strong lower-boundary current exists after $t = 1$. In late stages, this current becomes very narrow – though not as narrow as the porous-media case – and the location of the maximum of w_0 drops rapidly. Together with this, the density field develops a broad parabolic profile.

3.2. *Viscous diffusive flow*

We now consider viscous diffusive flow. Results are chiefly numerical. Both one-dimensional (channel) and two-dimensional (box) simulations are presented. Consideration is limited to ρ_2 being initially uniform and to $0 \leqslant R_D \leqslant R_\nu$. The two extreme cases $R_D = 0$ and $R_D = R_\nu$ will be seen to give qualitatively similar results. Time to frontogenesis seems to be set primarily by R_ν.

Figure 5 shows u_1, ρ_2 and the contour $\rho_2 x^2 = 10$ at time intervals of 0.4 for $R_\nu = 0.01$, $R_D = 0$. The flow evolution shown is qualitatively similar to that of all viscous cases examined. It can be seen that, even though R_D is zero and R_ν is small, the flow evolution becomes entirely different from the inviscid case. A major consequence of the viscous lower-boundary condition is that flows no longer remain stably stratified. Instead, it can be shown from (3.4*d*) that the position of maximum ρ_2 (starting from initially uniform ρ_2) must be in the interior and, further, once frontogenesis begins and w_0 is large, that it tends to be above the position of minimum u_1. An interior minimum u_1, of course, is created by the lower-boundary no-slip condition. Viscosity

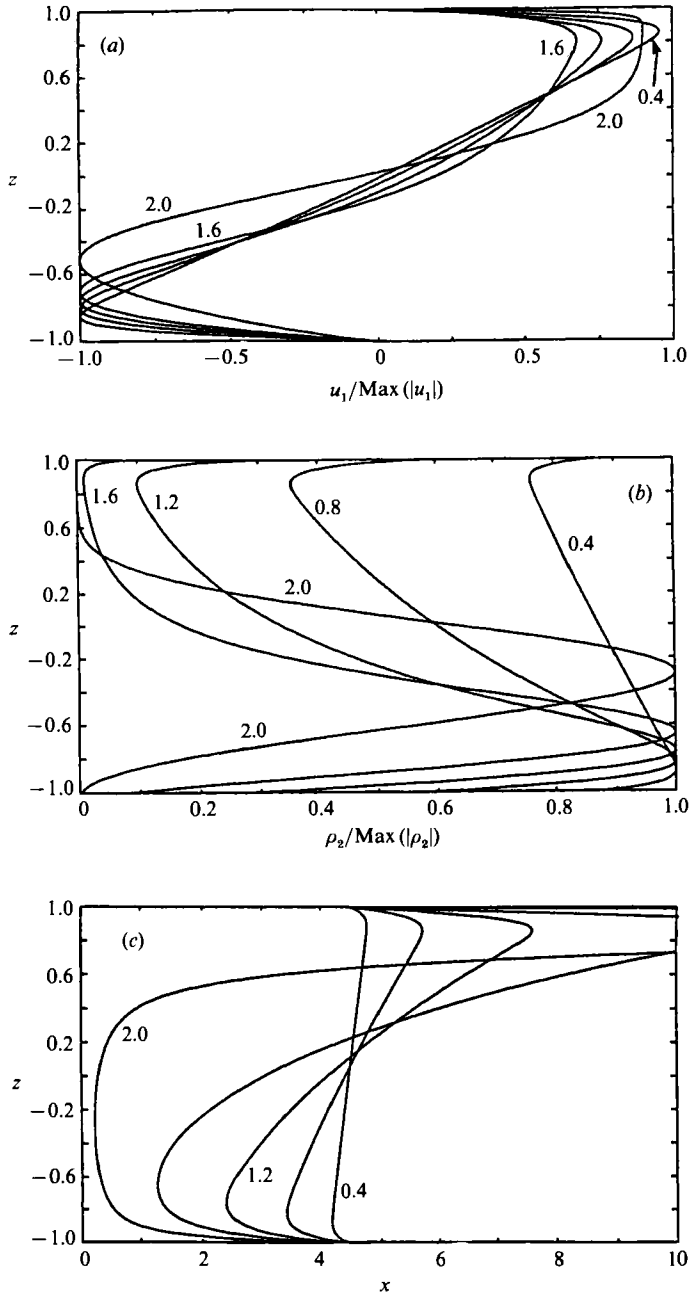

FIGURE 5. The Boussinesq case with $R_\nu = 0.01$, $R_D = 0$ with ρ_2 initially uniform. Scaled (*a*) u_1 and (*b*) ρ_2 and the contour (*c*) $\rho - \rho_0 = \rho_2 x^2 = 10$ are shown at time intervals of 0.4, from $t = 0.4$ to 2.

initially forces this minimum away from the boundary. Once away it is then forced by convection and by pressure effects to continue to rise. This inviscid interior forcing can be seen by checking the signs of the terms in (3.6). The viscous lower boundary condition thus leads, as the flow evolves, to a complete change in the dynamics of the interior flow.

Figure 6 details the late-time behaviour of the flow. At this point, calculations

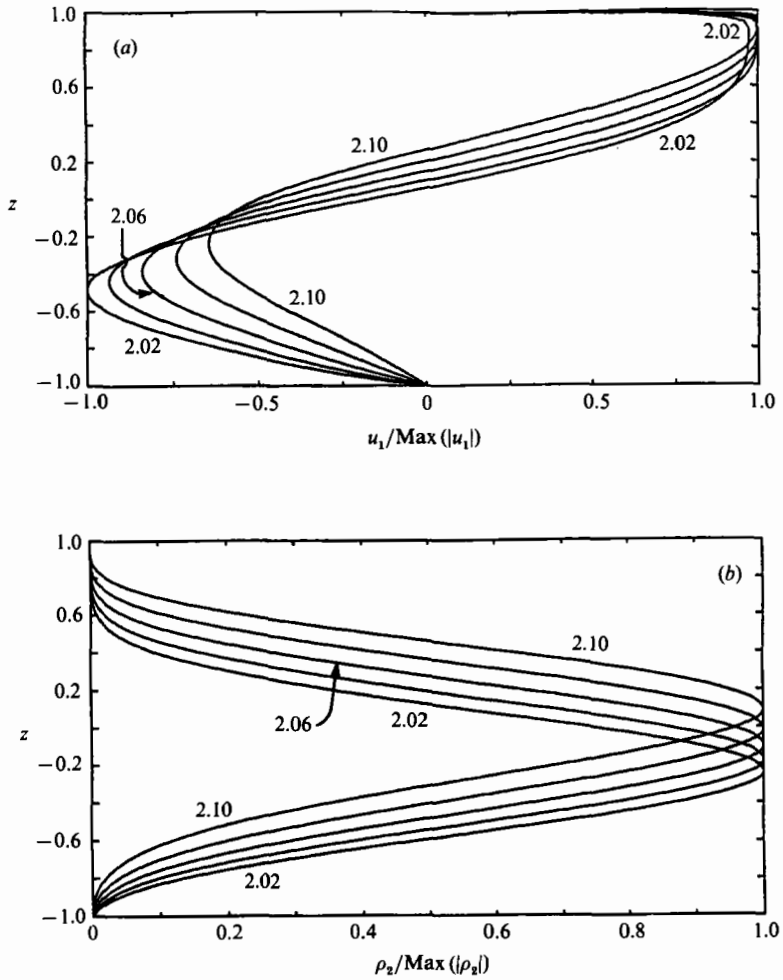

FIGURE 6. As for figure 5 but for late times, from $t = 2.02$ to 2.10 at time intervals of 0.02.

become rather difficult. Top and bottom boundary layers require increased grid resolution and both this increased grid resolution and the flow's great speed require very small time steps. At late times, the positions of maximum w_0, ρ_2, and minimum u_1 all rise very rapidly. One puzzling occurrence is the build-up of an upper-boundary current. This current becomes stronger than the lower-boundary frontal current. The character of the flow changes completely and results no longer have any bearing on *frontogenesis*.

Figure 7 shows a very diffusive case, $R_\nu = R_D = 0.1$. The results for ρ_2 are qualitatively similar to those shown in figure 5 though its top and bottom boundary layers are, of course, thicker and diffusion slows the initiation of frontogenesis. u_1 is viscously dominated until late times, keeping an approximately cubic profile ($u_1 \approx A(t)(z - z^3)$). An upper-boundary current forms starting at about $t = 3$. u_1 and ρ_2 grow very gradually up until about $t = 2$. Very rapid growth begins at about $t = 2.8$.

The occurrence of blow-up for the viscous case remains uncertain. All calculations made so far give monotonic and faster-than-exponential growth and have the appearance of leading to blow-up. However, because of time-step restrictions due to stability requirements, computations cannot actually be carried out to a blow-up. A

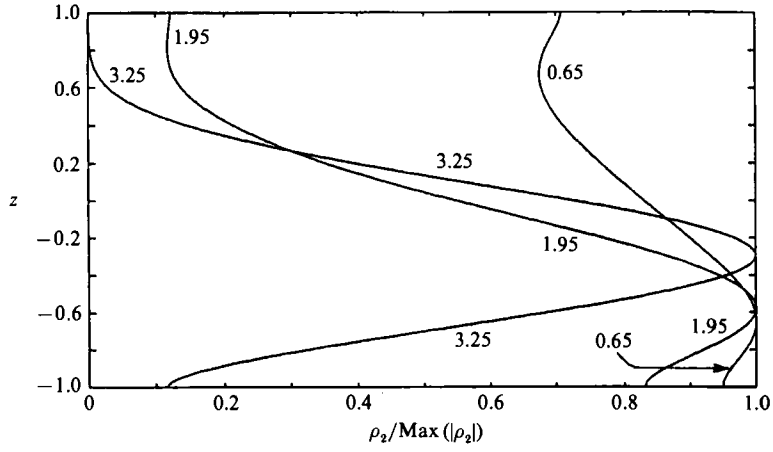

FIGURE 7. The Boussinesq case with $R_\nu = 0.1$, $R_D = 0.1$ with ρ_2 initially uniform. Scaled ρ_2 at times $t = 0.65$, 1.95, and 3.25.

$\rho_{\max}$	t
1	1.4007
10	2.8263
100	3.1574
1000	3.2566
10^4	3.2928
10^5	3.3085
10^6	3.3167
10^7	3.3216

TABLE 1. Increase of $\rho_{\max}(t)$ with t for $R_\nu = 0.1$, $R_D = 0.1$

rough extrapolation of the two cases discussed above gives rise an apparent time of blow-up for the first ($R_\nu = 0.01$, $R_D = 0$) of about 2.12 and for the second ($R_\nu = R_D = 0.1$) of about 3.33. An idea of the approach to the apparent blow-up for the second case is given in table 1. This gives t for selected values of $\rho_{\max}(t)$ ($\rho_{\max}$ increases monotonically with time). Extensive cross-checking has been done in an attempt to eliminate false blow-ups due to numerical problems. Both cases discussed above have been computed with various different time-step selection criteria, different spatial mesh sizes, and different finite-difference algorithms. Agreement holds amongst the various calculations to all times calculated. The data in table 1 were computed using 1600 mesh points, and from comparison to calculations with 800 and 400 mesh points, the results are accurate to at least six figures.

One rather nagging question was whether these channel results could be applied to finite geometries, in particular to the box geometry used by Simpson & Linden. It seemed likely that results would be applicable because the horizontal pressure gradient is determined locally (in x) through the hydrostatic pressure balance as long as ρ is locally horizontally quadratic. Thus, the evolution of the fluid at a point at the light end of the box should be independent of the circulation and mixing that occurs at the dense end until the recirculation penetrates close by. Recirculation at the light end is already included in the channel model. The only new feature there is the no-slip condition at $x = 0$. The effects of this, however, were expected to be confined to a narrow boundary layer.

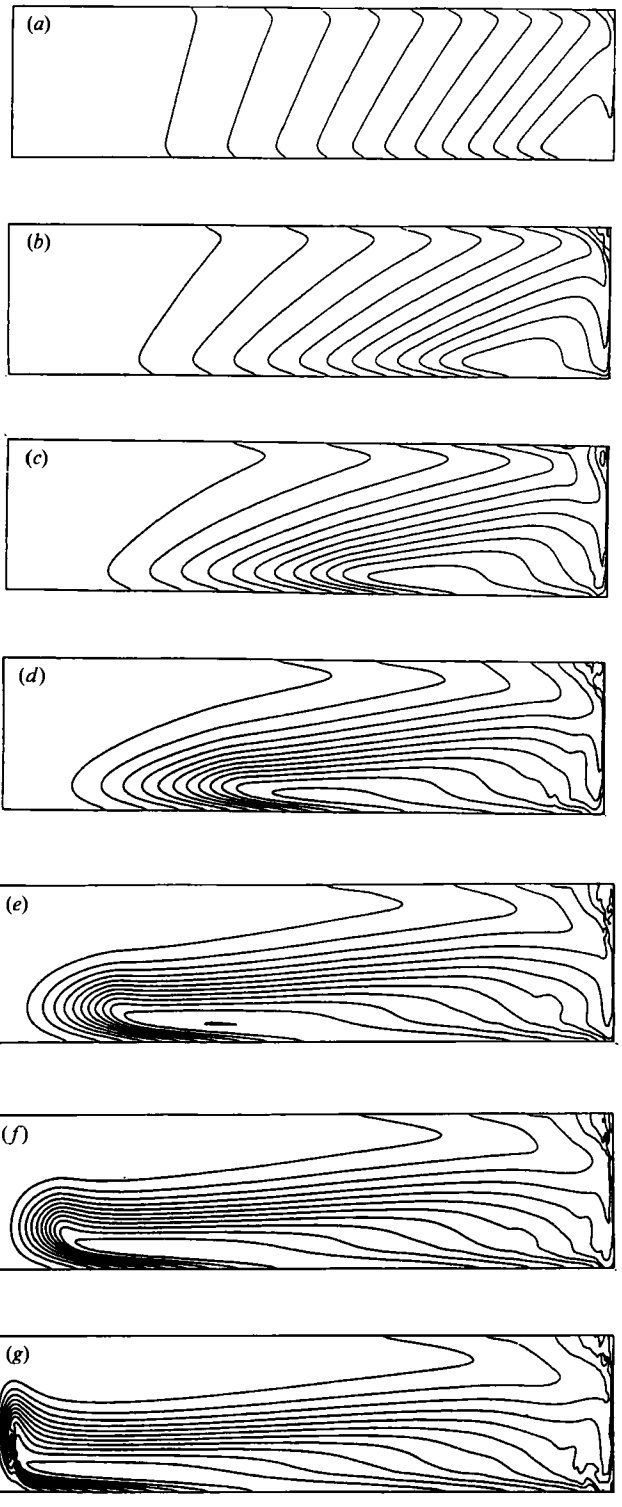

FIGURE 8. $\rho-\rho_0$ for the box calculation. Contours are at intervals of 0.02. Non-dimensional times shown are (*a*) 0.48, (*b*) 0.80, (*c*) 1.12, (*d*) 1.44, (*e*) 1.76, (*f*) 1.92, (*g*) 2.08.

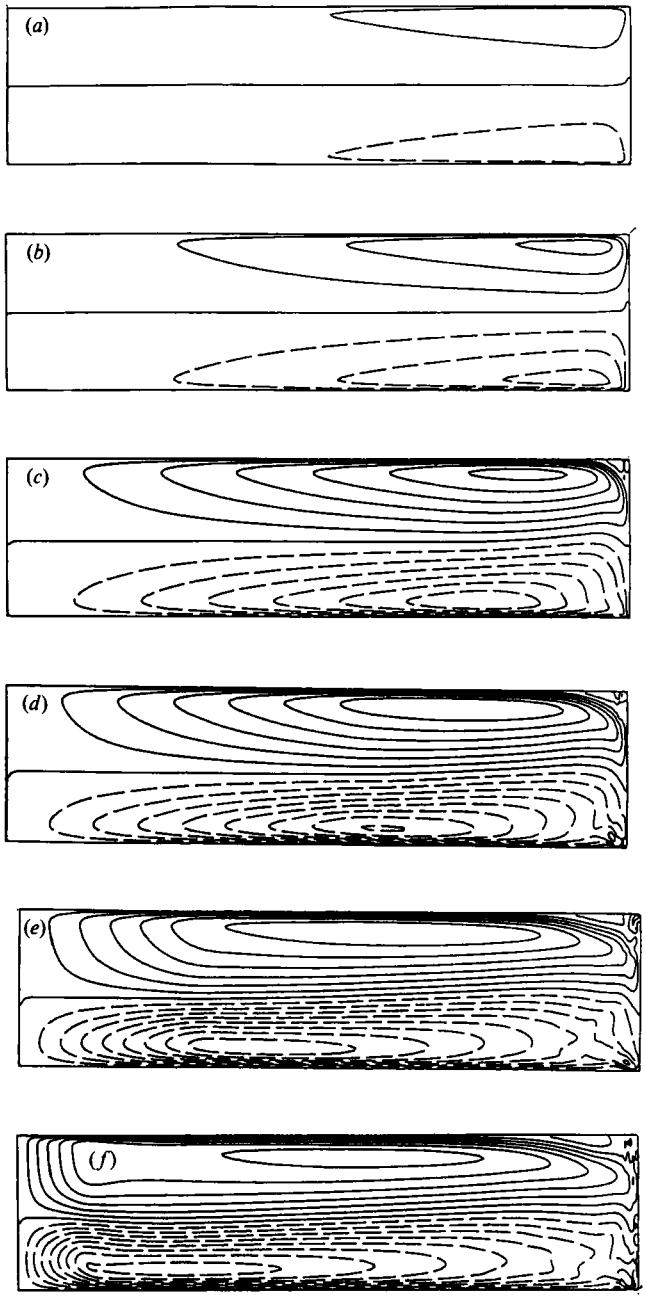

FIGURE 9. u for the box calculation. Contours are at intervals of 2 cm/s. Dashed contours indicate leftward velocity. Non-dimensional times shown are (*a*) 0.16, (*b*) 0.32, (*c*) 0.80, (*d*) 1.12, (*e*) 1.60, (*f*) 1.92.

To check all this, two-dimensional calculations were done of flow in a box. The calculations were dimensional. The box was taken to be 72 cm long and 3 cm high, the Earth's gravity was approximated as 1000 cm/s^2, and the initial dimensional ρ_2 was set to 0.000 05 g/cm^2. The calculations were meant to simulate a possible miniature version of the Simpson & Linden experiments, which were carried out in a box 3.6 m long and 15 cm high, or 5 times the size assumed for the simulation. The

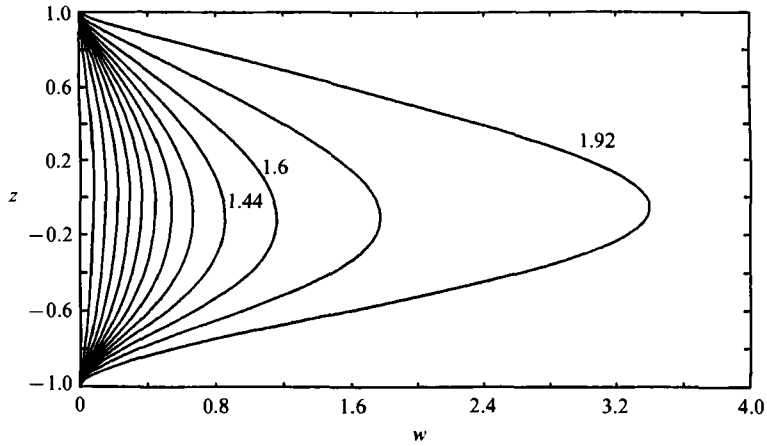

FIGURE 10. w for the box calculation at $x = 2$. Non-dimensional times shown are intervals of 0.16 from $t = 0.16$ to 1.92.

viscosity was set to ≈ 0.00871 cm^2/s. This choice yields an R_ν of 0.01. Two calculations were done with different diffusivities. In the first, the diffusivity was set equal to the viscosity ($R_D = 0.01$), in the second, to one-tenth the viscosity ($R_D = 0.001$). The second choice is more realistic (for water with density gradients due to temperature differences) but the first choice can be computed more reliably. The overall results for the two cases turned out to be very similar. One-dimensional channel flow calculations yield a non-dimensional apparent blow-up time for the first case of about 2.28 and for the second case of about 2.24. (To facilitate comparisons all times given in the ensuing discussion will be non-dimensional. Dimensional times in seconds can be found from the non-dimensional by dividing by $(0.15)^{\frac{1}{2}} \approx 0.3783$.) The channel flows lose their frontogenetic character, the upper-boundary current becoming dominant, at about $t = 2.05$ for the first case and $t = 2.03$ for the second. The calculations were done on a 960 by 60 uniform mesh using second-order space and time differencing.

Figures 8 and 9 show the evolution of ρ and u for the first case up to the non-dimensional time of 2.08. As observed with the channel calculations, u in the interior first develops into an approximately z-independent shear. The density field tilts with only a slight intensification of gradients. Frontogenesis begins after about $t = 1$. u loses its antisymmetry in z, its lower boundary current becoming dominant. At late times, in agreement with the channel calculations, this current begins to lift away from the channel floor (see figure 9*f*). Near the lower boundary density gradients intensify by close to an order of magnitude. At the upper, horizontal divergence nearly eliminates them. The channel-flow-like region in which these events occur shrinks with time, of course, but density remains nearly quadratic at the 'nose' of the boundary current up to about $t = 1.95$. The extent of the channel-flow-like region at any of the times shown can be deduced from the plots of u – in the channel-like region its contours are equispaced in the x-direction. For example, at $t = 1.76$ the region extends to about $x = 12$. Figure 10 shows w from the box calculation at $x = 3$ up to the non-dimensional time of 1.92. To the eye, plots of w from the channel and box calculations are in complete agreement up to the last time shown. At $t = 1.92$, the channel and box flow results disagree by less than 3%.

As mentioned above, the calculation with $R_D = 0.001$ gives generally very similar results. One interesting difference is the generation of a small patch of 'turbulence',

beginning at about $t = 1.6$, that follows behind the nose of the front. This, however, has no noticeable effect on flow profiles at the nose. These profiles agree with the channel flow calculations up to about $t = 1.92$.

Other box calculations, not discussed here, have also been done. These all show very good agreement with their corresponding channel calculations. What was surprising is how precise this agreement can be and how long it can last.

4. Discussion

We have presented two simple flow models that yield frontogenesis and that illustrate its essential dynamics in a clear-cut way. Both the porous-media model and the inviscid–non-diffusive Boussinesq model allow a wealth of exact results. Further, the Boussinesq model has been shown to be applicable to contained two-dimensional Boussinesq flow and thus, we hope, to experiments.

However, the limitations of the models should also be noted. Most serious is the viscous Boussinesq model's inability to account for turbulence. The later stages of flow in this model – particularly the lifting of the current and density front far from the lower boundary – are unrealistic. In an experiment, of course, turbulence would develop as a consequence of three-dimensional instabilities. The inclusion of some kind of modelled 'turbulent mixing' would probably eliminate these simulations' unrealistic late-stage behaviour. The qualitative nature of both the porous-media and Boussinesq equations further limits results.

The blow-up of the porous-media and inviscid Boussinesq models extends and sheds some further light on the results of Childress *et al.* It seems to confirm their comment that conclusions drawn from these blow-ups must be made with care. Blow-up, though interesting, probably reveals little new physics. Instead, it seems to be just a consequence of the unboundedness of initial conditions. On the other hand, the box calculations have shown that blow-up does not invalidate a model. Box and channel results agree up to fairly late times.

Our results have largely confirmed Simpson & Linden's hypotheses. Except for large R_ν, the scaled time both to frontogenesis and to blow-up is $O(1)$. These models clearly show the role of density curvature in causing lower-boundary horizontal convergence and from thence frontogenesis.

Appendix A. Porous-media blow-up

We begin by proving that $\partial w_0/\partial z$ is monotonically decreasing and convex, i.e. that, for all t, (i) $\partial^2 w_0/\partial z^2 \leqslant 0$ and (ii) $\partial^3 w_0/\partial z^3 \geqslant 0$. Consideration is limited to $R_D = 0$ and to initial distributions of density that are both $\geqslant 0$ and stably distributed ($\mathrm{d}\rho/\mathrm{d}z \leqslant 0$).

We first consider the monotonicity of $\partial w_0/\partial z$. For $\rho \geqslant 0$, both ρ_0 and ρ_2 must be $\geqslant 0$. ρ is subject only to advection so, since it is initially $\geqslant 0$, it must remain $\geqslant 0$ for all t. Thus ρ_2 must remain $\geqslant 0$. Since $\rho_2 = -\frac{1}{2}\partial^2 w_0/\partial z^2$, $\partial^2 w_0/\partial z^2$ must therefore always be $\leqslant 0$. To prove $\partial^3 w_0/\partial z^3 \geqslant 0$ we consider its evolution equation:

$$\frac{\partial}{\partial t}\frac{\partial^3 w_0}{\partial^3 z} + w_0 \frac{\partial^4 w_0}{\partial z^4} - \frac{\partial w_0}{\partial z}\frac{\partial^3 w_0}{\partial z^3} = 2\left(\frac{\partial^2 w_0}{\partial z^2}\right)^2. \tag{A 1}$$

Neither the convective nor the $\partial w_0/\partial z$ term can change the sign of $\partial^3 w_0/\partial z^3$. Since the 'source' term on the right-hand side of (2.5) is necessarily $\geqslant 0$ and since $\partial^3 w_0/\partial z^3 \geqslant 0$ initially, necessarily $\partial^3 w_0/\partial z^3 \geqslant 0$ for all t.

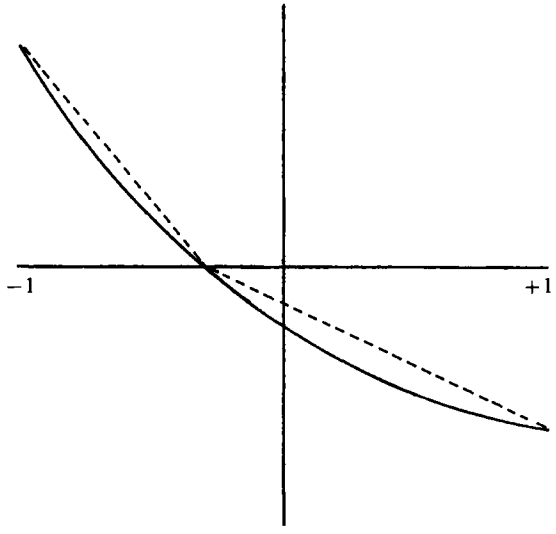

FIGURE 11. $\partial w_0/\partial z$ (solid line) and approximation (dashed line). The integral of this approximation is $\geqslant 0$.

Some additional characteristics of $\partial w_0/\partial z$ can be deduced from the fact that its integral is zero. From the monotonicity of $\partial w_0/\partial z$, $\partial w_0/\partial z|_{-1}$ is always positive and $\partial w_0/\partial z|_{+1}$ is negative. From its convexity, the location of $\partial w_0/\partial z = 0$ is in $z \leqslant 0$.

We now have enough information to prove blow-up. Integrating (2.4), the evolution equation for $\partial w_0/\partial z$ is

$$\frac{\partial}{\partial t}\frac{\partial w_0}{\partial z} + w_0\frac{\partial^2 w_0}{\partial z^2} - \frac{3}{2}\left(\frac{\partial w_0}{\partial z}\right)^2 = h(t); \tag{A 2}$$

$h(t)$ can be found in terms of $\partial w_0/\partial z$ by integrating (A 2). This yields

$$h(t) = -\frac{5}{4}\int_{-1}^{+1}\left(\frac{\partial w_0}{\partial z}\right)^2 \mathrm{d}z. \tag{A 3}$$

The evolution equation for $\partial w_0/\partial z$ at the lower boundary is

$$\frac{\partial}{\partial t}\frac{\partial w_0}{\partial z}\bigg|_{-1} = \frac{3}{2}\left(\frac{\partial w_0}{\partial z}\bigg|_{-1}\right)^2 + h(t). \tag{A 4}$$

Blow-up is proved by bounding $h(t)$ above $-\alpha(\partial w_0/\partial z|_{-1})^2$, where α is less than $\frac{3}{2}$.

The proof is in two parts. In the first part we bound the location of z_0, which is the value of z where $\partial w_0/\partial z$ equals zero. The convexity of $\partial w_0/\partial z$ has already led to $z_0 \leqslant 0$. It also leads to the ratio

$$-\frac{\partial w_0}{\partial z}\bigg|_{-1} \Big/ \frac{\partial w_0}{\partial z}\bigg|_{+1} = \beta \leqslant 1.$$

We now introduce a function that is everywhere $\geqslant \partial w_0/\partial z$. The function, shown in figure 11, is made up of two lines that intersect $\partial w_0/\partial z$ at $z = \pm 1$ and at z_0. Since the integral of $\partial w_0/\partial z = 0$, the integral of this function must be $\geqslant 0$. This leads to the desired lower bound for z_0. We find

$$-\frac{1-\beta}{1+\beta} \leqslant z_0 \leqslant 0. \tag{A 5}$$

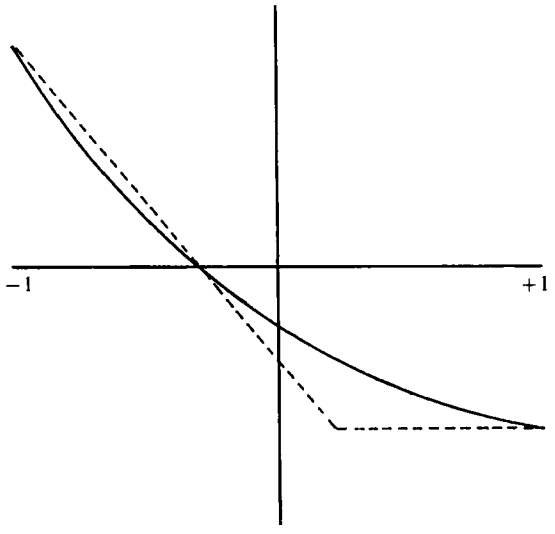

FIGURE 12. $\partial w_0/\partial z$ (solid line) and approximation (dashed line). The integral of the square of this approximation provides an upper bound on $\int_{-1}^{+1}(\partial w_0/\partial z)^2\,\mathrm{d}z$.

We now need an upper bound on the integral of $(\partial w_0/\partial z)^2$. The function

$$\mathrm{Max}\left[-\frac{\partial w_0}{\partial z}\bigg|_{-1}\frac{z-z_0}{z_0+1},\frac{\partial w_0}{\partial z}\bigg|_{+1}\right],$$

shown in figure 12, yields

$$\int_{-1}^{+1}\left(\frac{\partial w_0}{\partial z}\right)^2\mathrm{d}z \leqslant \mathrm{Max}\left[\left(\frac{\partial w_0}{\partial z}\bigg|_{-1}\right)^2((1+z_0)(1-\tfrac{2}{3}\beta^3)+(1-z_0)\beta^2)\right]. \tag{A 6}$$

Since the right-hand side of (A 6) is linear in z_0 the admissable maximum will be found at either $z_0 = 0$ or $z_0 = -(1-\beta)/(1+\beta)$. Calculations yield the maximum at the latter, at a β of about 0.86. We find

$$\int_{-1}^{+1}\left(\frac{\partial w_0}{\partial z}\right)^2\mathrm{d}z < 0.7114\left(\frac{\partial w_0}{\partial z}\bigg|_{-1}\right)^2. \tag{A 7}$$

An upper bound on the time to blow-up is now straightforward. Applying (A 7) to (A 4) gives

$$\frac{\partial}{\partial t}\frac{\partial w_0}{\partial z}\bigg|_{-1} > 0.6107\left(\frac{\partial w_0}{\partial z}\bigg|_{-1}\right)^2, \tag{A 8}$$

from which

$$\frac{\partial w_0}{\partial z}\bigg|_{-1} > \frac{\partial w_0/\partial z|_{-1,t=0}}{(1-0.6107\,\partial w_0/\partial z|_{-1,t=0}\,t)}. \tag{A 9}$$

Thus

$$t_\mathrm{b} < \left(0.6107\frac{\partial w_0}{\partial z}\bigg|_{-1,t=0}\right)^{-1}, \tag{A 10}$$

where t_b is the time to blow-up. Note that, from the convexity of $\partial w_0/\partial z$ and from the definition of A_ρ, $\partial w_0/\partial z|_{-1,t=0} \geqslant 1$. A global upper bound on t_b is thus 1.6375.

Appendix B. Boussinesq blow-up

As with the porous-media case, we must first consider some aspects of the flow's general behaviour. Consideration is limited to $R_\nu = R_D = 0$ and to flows that have $\rho \geqslant 0$ and that are initially motionless and stably stratified.

First, both p_2 and $\partial w_0/\partial z$ are monotonically decreasing and convex. The monotonicity of p_2 is due to the positivity of ρ_2. The monotonicity of $\partial w_0/\partial z$ can be proved from the evolution equation for $\partial^2 w_0/\partial z^2$. From (3.5$a$), this is

$$\frac{\partial}{\partial t}\frac{\partial^2 w_0}{\partial z^2} + w_0 \frac{\partial^3 w_0}{\partial z^3} - \frac{\partial w_0}{\partial z}\frac{\partial^2 w_0}{\partial z^2} = 2\frac{\partial p_2}{\partial z}. \tag{B 1}$$

$\partial^2 w_0/\partial z^2$ is initially zero but becomes negative because of the right-hand forcing. Neither the advection or $\partial w_0/\partial z$ term can then change the sign of $\partial^2 w_0/\partial z^2$. By similar reasoning it can next be shown that $\partial^2 p_2/\partial z^2 \geqslant 0$ always and then that $\partial^3 w_0/\partial z^3 \geqslant 0$.

Next, $\partial \overline{\rho_2}/\partial t \geqslant 0$ always. From the concavity of w_0 and from its boundary conditions, $w_0 \geqslant 0$ always. The equation for the evolution of $\overline{\rho_2}$, the z-averaged value of ρ_2, is

$$2\frac{\partial \overline{\rho_2}}{\partial t} = -\int_{-1}^{+1} w_0 \frac{\partial \rho_2}{\partial z}\,\mathrm{d}z + 2\int_{-1}^{+1} \rho_2 \frac{\partial w_0}{\partial z}\,\mathrm{d}z = 3\int_{-1}^{+1} w_0 \frac{\partial^2 p_2}{\partial z^2}\,\mathrm{d}z \tag{B 2}$$

which, since $\partial^2 p_2/\partial z^2 \geqslant 0$, must be $\geqslant 0$.

We now prove blow-up. With $R_\nu = 0$, (3.5a) at the lower boundary is

$$\frac{\partial}{\partial t}\frac{\partial w_0}{\partial z}\bigg|_{-1} - \left(\frac{\partial w_0}{\partial z}\bigg|_{-1}\right)^2 = 2p_2(-1). \tag{B3}$$

p_2 can be written as $\frac{1}{2}I(t) + \tilde{p}_2$, where

$$I(t) = -\int_{-1}^{+1} \left(\frac{\partial w_0}{\partial z}\right)^2 \mathrm{d}z, \quad \int_{-1}^{+1} \tilde{p}_2\,\mathrm{d}z = 0. \tag{B 4}$$

From the proof of blow-up for porous media, $I(t) > -0.7114(\partial w_0/\partial z|_{-1})^2$. Also, $\tilde{p}_2(-1) \geqslant \overline{\rho_2}$. This can be shown from the facts that (i) $\tilde{p}_2$ is convex, (ii) $\int_{-1}^{+1} \tilde{p}_2\,\mathrm{d}z = 0$, and (iii) $\tilde{p}_2(-1) - \tilde{p}_2(+1) = 2\overline{\rho_2}$. Since $\overline{\rho_2}$ is monotonically increasing, we have

$$\frac{\partial}{\partial t}\frac{\partial w_0}{\partial z}\bigg|_{-1} > 0.2886\left(\frac{\partial w_0}{\partial z}\bigg|_{-1}\right)^2 + 2\overline{\rho_2}(t_0) \tag{B 5}$$

for $t \geqslant t_0$. For $t_0 = 0$ this becomes, from the constraint on the initial value of $\overline{\rho_2}$,

$$\frac{\partial}{\partial t}\frac{\partial w_0}{\partial z}\bigg|_{-1} > 0.2886\left(\frac{\partial w_0}{\partial z}\bigg|_{-1}\right)^2 + 1. \tag{B 6}$$

Since $\partial w_0/\partial z$ is initially equal to zero, this yields

$$t_b < \frac{1}{(0.2886)^{\frac{1}{2}}}\frac{\pi}{2} \approx 2.924. \tag{B 7}$$

REFERENCES

CHILDRESS, S., IERLEY, G. R., SPIEGEL, E. A. & YOUNG, W. R. 1989 Blow-up of unsteady two-dimensional Euler and Navier–Stokes solutions having stagnation-point form. *J. Fluid Mech.* **203**, 1–22.

HOSKINS, B. J. & BRETHERTON, F. P. 1972 Atmospheric frontogenesis models: mathematical formulation and solution. *J. Atmos. Sci.* **29**, 11–37.

SIMPSON, J. E. & LINDEN, P. F. 1989 Frontogenesis in a fluid with horizontal density gradients. *J. Fluid Mech.* **202**, 1–16.

STUART, J. T. 1987 Nonlinear Euler partial differential equations: singularities in their solution. In *Symposium to Honor C. C. Lin.* World Scientific.